

Figure 5. Scanning electron micrograph of images generated by the isocyanate reversal process described in Scheme II. The imaging exposure was performed on a Perkin-Elmer Micralign 500 with approximately 15 mJ/cm². Sample was rinsed with 6:1 buffered HF for 2 s after etching.

viability of this approach but does not address the ultimate resolution capability of this image reversal scheme. The resolution limits of this dry-develop image reversal process have not been studied.

Concluding Remarks

Two key features underlie the approach to plasma developable resists outlined in Schemes I and II. The first is the photochemical generation of reactive functional groups within a polymeric film, and the second is the reaction of these functional groups with the proper chemical

reagent to ultimately obtain the desired oxygen plasma etch properties. If one desires an oxygen plasma etch barrier, then the chemical reagent should contain silicon, tin, germanium, or some other element that forms a refractory oxide. Correspondingly, if one desires the regions to be removed by etching, then one should use a chemical reagent composed of elements which form volatile oxides. The work described in this paper has used the acid-catalyzed generation of phenolic hydroxyl groups and the subsequent reaction with (dimethylamino)trimethylsilane or methyl isocyanate vapor to demonstrate this concept. However, the design concept contained in Schemes I and II should not be limited to just this small set of compounds. The synthetic chemical literature contains a variety of organometallic reagents, volatile organic reagents, and schemes designed to photochemically remove protecting groups.

In Schemes I and II, we have shown that the PBOCST/onium salt chemically amplified resist system can be dry-developed in an oxygen plasma to generate either a negative or a positive tone relief image. Previously, our laboratories have reported that the PBOCST/onium salt chemically amplified resist system can be developed with solvent to generate either a negative or positive tone relief image.^{22,23} Thus, the PBOCST/onium salt chemically amplified resist system is a remarkably versatile imaging system as it can be plasma developed, as well as solvent developed, to yield images of either tone.

Acknowledgment. We thank J. T. Hucko for editorial assistance and N. K. Voke for technical assistance.

Registry No. MIC, 624-83-9; TEA, 121-44-8; O₂, 7782-44-7; poly[4-((*tert*-butyloxycarbonyloxy)styrene)], 87261-04-9; triphenylsulfonium hexafluoroarsenate, 57900-42-2; (dimethylamino)trimethylsilane, 2083-91-2.

Synthesis and Characterization of Two New Quaternary Chalcogenides, CaYbInQ₄ (Q = S and Se), with an Olivine-Type Structure[†]

James D. Carpenter and Shiou-Jyh Hwu*

Department of Chemistry, Rice University, P.O. Box 1892, Houston, Texas 77251

Received July 24, 1992. Revised Manuscript Received September 18, 1992

Two new quaternary chalcogenide compounds, CaYbInQ₄ (Q = S and Se), were synthesized using a eutectic halide flux. The preliminary results from infrared spectroscopy experiments, using both DRIFTS and single-crystal transmittance methods, show no strong absorption bands in an extended infrared region (2–25 μm). These phases were structurally characterized by a single-crystal X-ray diffraction method. They crystallize in an orthorhombic crystal system with space group *Pnma* (No. 62) and *Z* = 4. The cell dimensions are *a* = 13.639 (2) Å, *b* = 7.926 (2) Å, *c* = 6.503 (2) Å, *V* = 703.1 (5) Å³ for the sulfide compound and *a* = 14.282 (3) Å, *b* = 8.247 (2) Å, *c* = 6.776 (1) Å, *V* = 798.1 (5) Å³ for the selenide compound. The single-crystal structure solutions of these chalcogenide analogues show that they adopt an olivine-type structure (Mg₂SiO₄). Structure refinements and chemical analysis suggest nonstoichiometry, which can possibly be attributed to cation mixing in an indium rich phase. The synthesis, structure characterization, and spectroscopy of the title compounds are discussed in this paper.

Introduction

The search for new materials with desirable optical properties has become important in recent years. In particular, a need has emerged for compounds that are

candidates for use as long-wavelength infrared (LWIR) window materials, e.g., 8–12 μm (a transparent region in the earth's atmosphere).^{1,2} It is apparent that there is a

[†] Presented at the inorganic chemistry poster session during the American Chemical Society Meeting, New York, NY, August 25–30, 1991.

* To whom correspondence should be addressed.

(1) (a) *Infrared Technology Fundamentals*; Spiro, I. J., Schlessinger, M., Eds.; Marcel Dekker, Inc.: New York, 1989. (b) *Window and Dome Technologies and Materials I*. Klocek, P., Ed.; *Proc. SPIE* 1989, 1112, and references therein. (c) *Window and Dome Technologies and Materials II*. Klocek, P., Ed.; *Proc. SPIE* 1990, 1326, and references therein.

deficiency of suitable materials which transmit in the infrared region and possess good thermal stabilities. This is because oxides and other strong ceramic materials have strong chemical bonds among light elements, causing vibrational excitation absorption bands that overlap with the desired infrared region. However, these ceramic materials display good thermal properties. Thus there is an inherent conflict (the chemical characteristics that give the best structural properties also tend to degrade the optical properties) which must be overcome in the search for advanced optical window materials.^{1c}

We are currently investigating rare-earth-metal-incorporated heavy post-transition-metal, quaternary chalcogenides for their potential as optical ceramic materials. Two new quaternary mixed-metal chalcogenides have been synthesized with a general formula of CaYbInQ_4 ($Q = \text{S}$ or Se). DRIFTS (diffuse reflectance infrared Fourier transform spectroscopy) and single-crystal transmittance infrared spectroscopy suggest that these compounds may show potential for device applications in the infrared region. Here we report the syntheses, X-ray single-crystal structures, and thermal properties of the two isostructural sulfide and selenide compounds, CaYbInQ_4 . We also report the preliminary results from infrared and UV-vis spectroscopy studies.

Experimental Section

Synthesis and Single-Crystal Growth. A two-step synthetic route was employed to prepare single crystals of the title compounds for analyses. Solid-state reactions were carried out for the preparation of the quaternary precursors, which use the starting materials CaQ ($Q = \text{S}$ and Se ; Aesar, 99.99% and 99.5%, respectively), Yb (Aldrich, 99.9%), In (Aldrich, 99.999%), and Q ($Q = \text{S}$ and Se ; Aldrich, 99.99% and Strem, 99.99%, respectively) in a molar ratio 1:1:1:3. The reaction mixtures were ground together under a blanket of nitrogen in a drybox and then loaded into quartz reaction ampules, which were subsequently sealed under vacuum. The mixtures were heated at a rate of 60 °C/h to a final temperature of 1000 °C, annealed at this temperature for 6 days, and then furnace cooled to room temperature. The polycrystalline materials obtained were examined by a powder X-ray diffraction method (showing largely a mixture of CaYb_2Q_4 and In_2Q_3) and then were used as starting materials for single-crystal growth experiments.

A molten salt technique has been used in the exploratory synthesis of rare-earth element (refractory metal) containing compounds.³ A mixed-halide CaCl_2/KCl eutectic flux was employed for the single-crystal growth of the title compounds. These halide salts, CaCl_2 (Johnson Matthey Inc., reagent) and KCl (Baker, reagent), were dried under vacuum at approximately 200 °C, then weighed in a drybox, and ground together prior to use. The composition of the eutectic flux was $\text{CaCl}_2:\text{KCl} \sim 74:26$ mol % (mp 640 °C).⁴ Crystal growth experiments were carried out in carbon-coated silica ampules, which were previously outgassed under vacuum. The ampules were loaded in a drybox with a mixture of the precursor and flux in a mass ratio of 1:4. The loaded ampules were held under active vacuum for 2.5 h prior to sealing. The reactant mixtures were heated to 1000 °C at a rate of approximately 60 °C/h held at this temperature for 6 days, cooled at a rate of 1.5 °C/h to 600 °C, and then cooled to room temperature over 24 h. Lime-green (CaYbInS_4) and brownish-orange (CaYbInSe_4) transparent crystals of the desired compounds were isolated from the flux by washing the reaction products with deionized water, using a suction filtration method. The observed

Table I. Crystallographic Data for CaYbInQ_4 ($Q = \text{S}$ and Se)

chemical formula	CaYbInS_4	CaYbInSe_4
formula mass (amu) ^a	438.89	634.13
space group	<i>Pnma</i> (No. 62)	<i>Pnma</i> (No. 62)
cell parameters ^b		
<i>a</i> (Å)	13.639 (2)	14.282 (3)
<i>b</i> (Å)	7.926 (2)	8.247 (2)
<i>c</i> (Å)	6.503 (2)	6.776 (1)
<i>V</i> (Å ³)	703.1 (5)	798.1 (5)
<i>Z</i>	4	4
<i>T</i> (K) of data collection	296	296
ρ_{calc} (g cm ⁻³) ^a	4.15	5.28
radiation (graphite monochromated)	Mo K α ($\lambda = 0.71069$ Å)	
crystal shape, color	octagonal plate, lime green	rectangular plate, brownish-orange
crystal size (mm)	0.5 × 0.2 × 0.1	0.3 × 0.2 × 0.2
linear abs coeff (cm ⁻¹)	181.60	330.59
transmission factors	0.72–1.00	0.39–1.00
scan type	ω scans	ω scans
scan speed (deg min ⁻¹)	4.00	4.00
scan range (deg)	–0.36 to 0.36	–0.45 to 0.45
background counts	1/4 of scan range on each side of reflection	
2 θ (max) (deg)	55	55
data collected	<i>h</i> , <i>k</i> , <i>l</i>	<i>h</i> , <i>k</i> , \pm <i>l</i>
no. of unique data (<i>I</i> > 0)	879	1104
no. of unique data with <i>I</i> > 3 σ (<i>I</i>)	717	684
F_{000} ^a	787	1086
R^c	0.023	0.041
R_w^c	0.030	0.050
R (<i>I</i> > 3 σ (<i>I</i>))		0.037
goodness of fit ^d	1.17	1.68
no. of variables	41 ^e	41 ^e

^a Calculated based upon the structural formulas of $\text{Ca}_{1.06}\text{Yb}_{0.78}\text{In}_{1.16}\text{S}_4$ and $\text{Ca}_{1.02}\text{Yb}_{0.86}\text{In}_{1.12}\text{Se}_4$. ^b The refinement of cell constants is constrained in orthorhombic crystal system. ^c $R = \sum(|F_o| - |F_c|) / \sum|F_o|$; $R_w = [\sum w(|F_o| - |F_c|)^2 / \sum w|F_o|^2]^{1/2}$. ^d The errors in the observed unit weight (e^2) are 2.05 and 2.34 for the sulfide and selenide phases, respectively. ^e The refined extinction coefficients are $5.7(4) \times 10^{-7}$ for sulfide and $2.4(3) \times 10^{-7}$ for selenide.

yield of the title compounds was approximately 50%. The major byproduct was CaYb_2Q_4 , according to powder X-ray diffraction patterns.

Structure Determination. The detailed crystallographic data for CaYbInQ_4 ($Q = \text{S}$ and Se) are listed in Table I. The routine data collection procedures were the same as previously reported.³ To prevent sample decomposition in air (see later discussion), a thin layer of epoxy was applied to protect the data crystals. The unit cell parameters and the orientation matrix for data collection were determined by a least-squares fit of 25 reflections ($6.94 \leq 2\theta \leq 20.24$ for the sulfide phase; $6.68 \leq 2\theta \leq 22.43$ for the selenide phase). In both cases, there was no detectable decay of the intensities of three standard reflections (0,–1,1; 1,–3,1; 0,–3,1 for the sulfide and 0,–4,2; 0,–4,–1; 2,–6,0 for the selenide) which were measured every 150 reflections during data collection. Lorentz–polarization and empirical absorption corrections, based on azimuthal scans ($2\theta = 11.91, 21.53$, and 23.44 for $Q = \text{S}$; $2\theta = 19.85, 20.67$, and 31.15 for $Q = \text{Se}$), were applied to the intensity data. On the basis of the Laue symmetry (*mmm*), intensity statistics, and the successful solution and structure refinement, the space group was determined to be *Pnma* (No. 62). The atomic coordinates for the selenide phase were found by the PATTERSON method using the program SHELXS-86.⁵ The structural and anisotropic thermal parameters of the CaYbInSe_4 phase were then refined by full-matrix least-squares methods based on *F* to *R* = 0.050, $R_w = 0.067$, and GOF = 2.24, using the TEXSAN software package.⁶ The occupancy factors for all the atoms in the structure were initially refined, but the resultant value indicated non-stoichiometry only on the calcium and ytterbium sites. The structure refinement of the sulfide phase was based on the atomic coordinates derived from its selenide analogue. It too proved to

(2) Johnson, C. E.; Vanderah, T. A.; Bauch, C. G.; Harris, D. C. In *Ceramics and Inorganic Crystals for Optics, Electro-Optics, and Nonlinear Conversion*. Proc. SPIE 1988, 968, 41.

(3) (a) Carpenter, J. D.; Hwu, S.-J. *J. Solid State Chem.* 1992, 97, 332. (b) Carpenter, J. D.; Hwu, S.-J. *Acta Crystallogr.* 1992, C48, 1164.

(4) Phase Diagrams for Ceramists; Vol. II, Levin, E. M., Robbins, C. R., McMurdie, H. F., Eds.; The American Ceramic Society Inc.: Columbus, OH, 1969; Figure 3054.

(5) Sheldrick, G. M. In *Crystallographic Computing 3*, Sheldrick, G. M., Krüger, C., Goddard, R., Eds.; Oxford University Press: London, 1985; pp 175–189.

(6) TEXSAN: Single Crystal Structure Analysis Software, version 5.0. Molecular Structure Corp.: The Woodlands, TX, 1989.

Table II. Atomic Coordinates and Thermal Parameters for CaYbInQ₄ (Q = S and Se)

atom	x	y	z	B _{eq} (Å ²) ^c
CaYbInS ₄ ^a				
Ca	0.2692 (1)	1/4	0.9941 (2)	1.12 (5)
Yb	1/2	0	1/2	1.03 (2)
In	0.08922 (5)	1/4	0.4163 (1)	1.14 (2)
S(1)	0.0866 (2)	1/4	0.7860 (3)	1.08 (7)
S(2)	0.4279 (1)	1/4	0.2649 (3)	1.20 (8)
S(3)	0.1609 (1)	0.0075 (2)	0.2357 (2)	1.24 (6)
CaYbInSe ₄ ^b				
Ca	0.2668 (2)	1/4	0.9973 (6)	1.5 (1)
Yb	1/2	0	1/2	1.22 (4)
In	0.0874 (1)	1/4	0.4111 (2)	1.33 (6)
Se(1)	0.0869 (2)	1/4	0.7837 (3)	1.21 (8)
Se(2)	0.4251 (2)	1/4	0.2673 (4)	1.36 (8)
Se(3)	0.1616 (1)	0.0046 (2)	0.2348 (2)	1.32 (6)

^aThe multiplicities for the final refinements are 0.42 and 0.08 for calcium and indium on the Ca site, 0.39 and 0.11 for ytterbium and calcium on the Yb site, respectively. ^bThe multiplicities for the final refinements are 0.44 and 0.06 for calcium and indium on the Ca site, 0.43 and 0.07 for ytterbium and calcium on the Yb site, respectively. ^cAnisotropically refined atoms are given in the form of the isotropic equivalent displacement parameters defined as $B_{eq} = (8\pi^2/3) \text{tr } U$.

be a nonstoichiometric phase (see later discussion). A correction for the secondary extinction⁷ was applied and resulted in a better least-squares solution, as shown by the improved $\Delta F/\sigma F$ values on reflections having $\Delta F/\sigma F > 10$ (0,4,0 for Q = S; 0,2,0; 0,4,0; 4,0,0 for Q = Se). The final positional and isotropic thermal parameters are given in Table II.

Wavelength Dispersive Spectroscopy (WDS) Analysis. The estimated chemical composition of the CaYbInS₄ data crystal was determined using wavelength-dispersive spectroscopy. A Cameca SX-50 electron microprobe was used to perform the experiment. Data acquisition was accomplished using four scanning spectrometers. The intensities of each of the X-ray emissions of the sample were compared with those of a standard. The standards used for the analyses were Wollastonite,^{8a} rare-earth glass standard no. 2,^{8b} InAs (Tousimis), and Pyrite (Tousimis). The normalized formula of the sulfide phase showed an indium-rich composition of Ca:Yb:In:S = 1.0:0.8:1.4:4. Quantitative chemical analysis could not be conducted on the selenide phase due to its moisture sensitivity.

Powder X-ray Diffraction. Ground single crystals of the title compounds were analyzed at room temperature using a powder X-ray diffraction (XRD) technique on a Phillips PW 1840 Diffractometer (with Cu K α radiation, Ni filter). NBS (National Bureau of Standards) silicon was mixed with the samples and used as an internal standard. The diffraction patterns obtained ($10^\circ \leq 2\theta \leq 60^\circ$) were indexed and refined by the least-squares program LATT⁹ with constraint to the orthorhombic crystal system. All observed (28) reflections were able to be indexed and the refined lattice parameters (below) are in good agreement with those obtained from the single crystal data (see Table I):

	CaYbInS ₄	CaYbInSe ₄
a (Å)	13.654 (6)	14.279 (3)
b (Å)	7.921 (5)	8.2477 (8)
c (Å)	6.496 (2)	6.776 (1)

Thermal Analysis. The thermal analysis of the title compounds was performed using a Du Pont 9900 Thermal Analysis System. The investigations were conducted on ground selected single-crystal samples (~15 mg). The thermogravimetric analysis (TGA) experiments on the sulfide and selenide samples, which were contained in a platinum pan, showed that these compounds

were stable in a pure oxygen atmosphere up to 575 °C (the onset decomposition point) for the sulfide phase and 715 °C for the selenide phase. The value for ZnS is ca. 600 °C.¹⁰ These values are higher than those found for the ternary post-transition-metal chalcogenides: Ca_{3.3}In_{6.5}S₁₃ (375 °C), Ca_{1.2}In_{1.9}S₄ (425 °C), SrIn₂S₄ (425 °C), BaIn₂S₄ (425 °C).¹¹ The higher decomposition temperature is probably, in part, due to the incorporation of rare-earth elements. Furthermore, both phases were examined by differential thermal analysis (DTA) in sealed quartz ampules (~15 mg) under vacuum. Neither phase transitions nor melting phenomena were observed up to ~1250 °C. The DTA samples were examined by powder X-ray diffraction after the experiment and showed that the compounds remained intact.

Infrared and UV-Vis Spectroscopy. Both the sulfide and selenide phases were examined spectroscopically. The infrared spectra of the title compounds were obtained from diffuse reflectance infrared Fourier transform spectroscopy (DRIFTS) and single-crystal transmittance infrared spectroscopy. The DRIFTS experiments on polycrystalline samples were performed using an IBM-98 FT-IR spectrometer which was equipped with a set of DRIFTS optics (Analect). After the application of the Kubelka-Munk function,¹² the obtained spectra (4000–400 cm⁻¹) showed only weak absorption bands due to water in the investigated range.

Preliminary single-crystal infrared transmittance investigations of CaYbInS₄ were performed using a SPECTRA TECH IR-PLAN spectrometer equipped with a microscope. Spectra were taken on plate crystals (ca. 0.4 mm × 0.4 mm × 0.1 mm) of the title compound which were placed on a KBr plate. A 32 times magnification head, with an aperture size of 26 × 26 μm, was used during the study. 250 scans from 5000 to 625 cm⁻¹ (2–16 μm) with a resolution of 2 cm⁻¹ were used for both the sample and reference (KBr plate) spectra. In this spectrum two weak absorption bands and many interference fringes are observed. The absorption bands, which are attributed to the water used to isolate crystals from the flux, can be assigned to symmetric/antisymmetric O–H stretching (2.91 μm) and to H–O–H bending (6.20 μm).¹³ However, it should be noted that there is an inherent loss in the signal/noise ratio¹⁴ using this method. Therefore, high-resolution single-crystal infrared transmittance spectroscopy is under investigation.

The title compounds were also investigated in the UV-vis region by reflectance spectroscopy. A Hitachi 330 spectrometer, fitted with an integrating sphere, was used to conduct the reflectance measurements from 2500 to 250 nm. Half-inch pellets of the title compounds, made from ground single crystals, were used for the measurements. The spectrum of BaSO₄ was taken as a reference standard for the experiments. The obtained spectra were interpreted using methods previously described by Schevciw et al.¹⁵ The results of these investigations suggest bandgaps of ca. 2.0 and ca. 1.7 eV for CaYbInS₄ and CaYbInSe₄, respectively.

Structure Description and Discussion

Nonstoichiometry is a common phenomenon observed in ternary chalcogenides which contain alkaline-earth and

(10) Covino, J. In *Advanced Optical Materials. Proc. SPIE 1984, 505, 42.*

(11) (a) Kipp, D. O.; Lowe-Ma, C. K.; Vanderah, T. A. *Chem. Mater.* 1990, 2, 506. (b) Lowe-Ma, C. K.; Kipp, D. O.; Vanderah, T. A. *J. Solid State Chem.* 1991, 92, 520.

(12) The Kubelka-Munk (KM) function, $F(R_\infty)$, is used to describe the behavior of diffuse reflectance in the mid-IR region. The KM function is given by

$$F(R_\infty) = (1 - R_\infty)^2 / 2R_\infty = k/s$$

where R_∞ is the diffuse reflectance transmittance spectrum of an infinitely thick sample which is ratioed to the spectrum of a nonabsorbing reference, k is the absorption coefficient, and s is the scattering coefficient. The KM function is the diffuse reflectance analog of the Beer-Lambert law for transmittance measurements, as such the KM function should be used when analyzing spectra that are collected with DRIFTS. (a) Kubelka, P.; Munk, F. Z. *Tech. Phys.* 1931, 12, 593. (b) Kubelka, P. *J. Opt. Soc. Am.* 1948, 38, 448.

(13) Nakamoto, K. *Infrared and Raman Spectra of Inorganic and Coordination Compounds*, 4th ed.; Wiley-Interscience Publication: New York, 1986; p 228.

(14) Nadler, M. P.; Lowe-Ma, C. K.; Vanderah, T. A. *Mater. Res. Bull.*, submitted.

(15) Schevciw, O.; White, W. B. *Mater. Res. Bull.* 1982, 18, 1059.

(7) Zachariasen, W. H. *Acta Crystallogr.* 1968, A24, 212.

(8) (a) Analytical Laboratory Report No. 72-WO-3. United State Geological Survey, 1972. (b) Drake, M. J.; Weill, D. F. *Chem. Geol.* 1972, 10, 179.

(9) LATT: F. Takusagawa, Ames Laboratory, Iowa State University, Ames, Iowa, unpublished research, 1981.

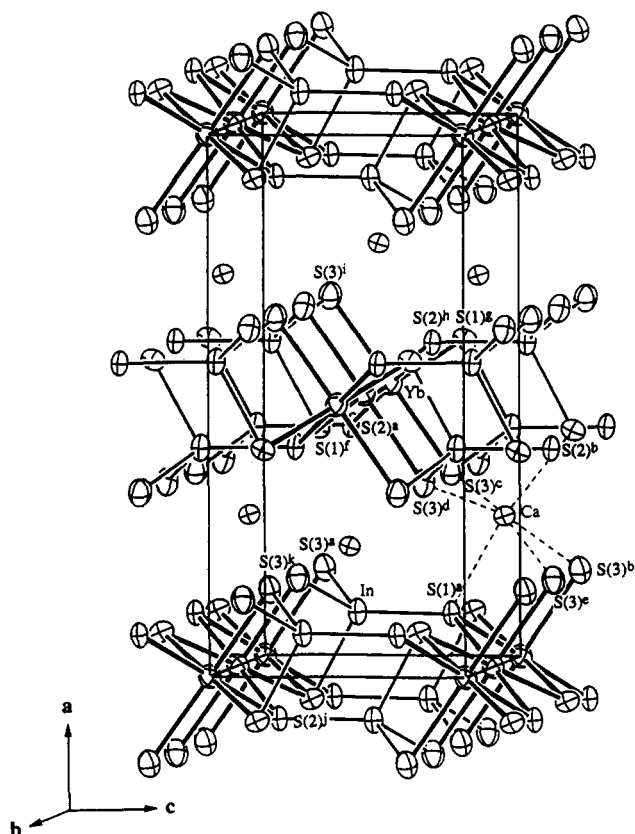


Figure 1. ORTEP drawing of the structure of CaYbInQ_4 reviewed approximately along the b axis. The anisotropic thermal ellipsoids are presented in 90% probability. The YbS_6 octahedral coordination is drawn in thick lines, while the InS_4 tetrahedral coordination is drawn in thin lines. The octahedrally coordinated CaS_6 is outlined by dashed lines. See Table III for symmetry codes.

rare-earth metal cations. Nonstoichiometry has been evident in these chalcogenide phases due to cation mixing, i.e., $\text{Ca}_{1-x}\text{Yb}_{2+x}\text{S}_4$ ^{3a} or cation and anion deficiencies, e.g., $\text{Ba}_{1-x}\text{Sm}_2\text{S}_{4-x}$.^{3b} In the presently studied phases, the multiplicities for the calcium and ytterbium atoms were originally refined with fixed thermal parameters to be 0.62 and 0.42 for the sulfide compound and 0.59 and 0.45 for the selenide compound, respectively (vs 0.5 for a fully occupied site). The calculated structure formulas (see Table I) are based upon the final refinements with confined multiplicities.¹⁶ The refined stoichiometry showed a consistency with the values obtained from WDS analysis. These results suggest that the title compounds are nonstoichiometric due to cation mixing in an indium-rich phase. Subsequent attempts to synthesize either stoichiometric or nonstoichiometric compounds below 1200 °C, however, have resulted in multiple phases, as determined by powder X-ray methods. We speculate that higher temperatures may be required to form the title

(16) The general structural formula is assumed to be $\text{Ca}_{1-x+y}\text{Yb}_{1-y}\text{In}_{1+x}\text{Q}_4$. The final refinements were carried out with confined multiplicities, i.e., the six-coordinated calcium cation sites were simultaneously occupied by indium cations, while the ytterbium sites were simultaneously occupied by calcium cations. The multiplicities were originally refined with fixed isotropic thermal parameters, i.e., $\text{Ca}/\text{Yb} = 0.89/1.08$ and $1.4/1.23$ for the sulfide and selenide phases, respectively. The final refinements were accomplished with varied thermal parameters while the resultant multiplicities were fixed. The calculated x and y values are 0.16 and 0.22 for the sulfide phase and 0.12 and 0.14 for the selenide phase, respectively. It should be noted that nonstoichiometry with respect to different combinations of cation mixing is possible.

compounds. The stoichiometric structure formula, CaYbInQ_4 , is used hereafter for convenience in the structural description.

The title compounds, CaYbInQ_4 ($Q = \text{S}$ and Se), crystallize in orthorhombic unit cells. In Figure 1, the ORTEP¹⁷ drawing shows the contents of the unit-cell structure of the sulfide compound, which is viewed approximately along the b axis. The unit cell is drawn slightly tilted so that the octahedrally coordinated YbS_6 and the tetrahedrally coordinated InS_4 may be discerned. The octahedral coordination of the calcium atom is outlined by dashed lines. The overall lattice is shown to be a 3D structure which consists of approximately hexagonal close-packed layers of Q^{2-} ions ($Q = \text{S}$ and Se), lying in sheets nearly parallel to the (100) plane.

Although there are many oxide compounds with the olivine structure there are relatively few chalcogenide, especially selenide, compounds of this type.¹⁸ These quaternary chalcogenides are isostructural with olivine (Mg_2SiO_4),¹⁹ with the Yb^{3+} (4a) and Ca^{2+} (4c) cations in the independent magnesium sites and the In^{3+} (4c) cations in the silicon sites. In one interstitial layer half of the octahedral sites are occupied by Yb^{3+} ions and one-quarter of the tetrahedral sites are occupied by the In^{3+} ions. In the other interstitial layers, half of the octahedral sites are occupied by Ca^{2+} ions and the tetrahedral sites are vacant. This atomic arrangement leads to a structural formula of CaYbInQ_4 .

The structure of these quaternary chalcogenides can be considered as a layered type in which the chalcogenide $[\text{YbInQ}_4]^{2-}$ slabs are stacked along the crystallographic a axis, with calcium cations in the octahedral interstitial sites. The layered characteristics can be justified by the difference in the bonding nature of the largely covalent $[\text{YbInQ}_4]^{2-}$ slabs vs primarily ionic interstitial layers of Ca^{2+} . In fact, the selenide compound is moisture sensitive, i.e., the compound reacts with moisture resulting in a volume expansion and eventually total decomposition. It is interesting to observe that the selenide single crystals start to delaminate in a water solution. The sulfide compound, on the other hand, seems to be less moisture sensitive. Compared with the selenide analogue, the extra stability in the sulfide compound is possibly attributed to the stronger interlayer electrostatic interaction between sulfide slabs.

Table III shows that the bond distance range for the covalently bonded Yb-Q and In-Q is relatively narrow, e.g., 2.68–2.69 Å (Yb-S), 2.41–2.50 Å (In-S), 2.80–2.82 Å (Yb-Se), and 2.53–2.61 Å (In-Se), so is the bond distance range for the ionically bonded Ca-Q , e.g., 2.79–2.89 Å (Ca-S) and 2.91–2.99 Å (Ca-Se). These bond distances are all comparable with the sum of the Shannon crystal radii,²⁰ as listed in Table III, as well as those in known phases, such as 2.66–2.77 Å (Yb-S) in CaYb_2S_3 ^{3a} and 2.42–2.48 Å (In-S , 4CN) in KInS_2 ^{12b} and 2.47–2.91 Å (In-S , 6CN) in $\text{Ca}_{3.1}\text{In}_{6.6}\text{S}_{13}$.²¹ It is noted that the small deviation in bond angles suggests that the YbQ_6 and CaQ_6 octahedra and the InQ_4 tetrahedra are slightly distorted.

In the $[\text{YbInQ}_4]^{2-}$ slab, the YbO_6 octahedra share opposite edges to form an infinite chain along the b axis,

(17) Johnson, C. K. ORTEP II. Report ORNL-5138. Oak Ridge National Laboratory, Tennessee, 1976.

(18) Pearson's Handbook of Crystallographic Data for Intermetallic Phases, 2nd ed.; Villars, P., Calvert, L. D., Eds.; ASM International: Materials Park, OH, 1991; p 232.

(19) Rock-Forming Minerals. Orthosilicates, Deer, W. A., Howie, R. A., Zussman, J. Eds.; Longman: London, 1982; Vol. 1A.

(20) Shannon, R. D. Acta Crystallogr. 1976, A32, 751.

(21) Chapuis, G.; Niggli, A. J. Solid State Chem. 1972, 5, 126.

Table III. Selected Bond Distances (Å) and Angles (deg) for CaYbInQ₄ (Q = S and Se)^a

	CaYbInS ₄	CaYbInSe ₄
YbQ ₆		
Yb-Q (1) ^{f,g}	2.694 (2) (2×)	2.818 (2) (2×)
Yb-Q (2) ^{a,h}	2.689 (2) (2×)	2.807 (2) (2×)
Yb-Q (3) ^{c,i}	2.677 (2) (2×)	2.804 (2) (2×)
Q (1) ^f -Yb-Q (1) ^g	180.00	180.00
Q (1) ^{f,g} -Yb-Q (2) ^{a,h}	95.06 (5) (2×)	94.44 (5) (2×)
Q (1) ^{f,g} -Yb-Q (2) ^{h,a}	84.94 (5) (2×)	85.56 (5) (2×)
Q (1) ^{f,g} -Yb-Q (3) ^{c,i}	85.44 (6) (2×)	85.56 (5) (2×)
Q (1) ^{f,g} -Yb-Q (3) ^{i,c}	94.56 (6) (2×)	94.44 (5) (2×)
Q (2) ^a -Yb-Q (2) ^h	180.00	180.00
Q (2) ^{a,h} -Yb-Q (3) ^{c,i}	92.44 (5) (2×)	90.86 (6) (2×)
Q (2) ^{a,h} -Yb-Q (3) ^{i,c}	87.56 (5) (2×)	89.14 (6) (2×)
Q (3) ^c -Yb-Q (3) ⁱ	180.00	180.00
InQ ₄		
In-Q (1) ^a	2.405 (2)	2.525 (3)
In-Q (2) ^j	2.496 (2)	2.614 (3)
In-Q (3) ^{a,k}	2.455 (2) (2×)	2.578 (2) (2×)
Q (1) ^a -In-Q (2) ^j	117.32 (8)	117.4 (1)
Q (1) ^a -In-Q (3) ^{a,k}	118.95 (5) (2×)	117.68 (6) (2×)
Q (2) ^j -In-Q (3) ^{a,k}	97.19 (5) (2×)	98.65 (6) (2×)
Q (3) ^a -In-Q (3) ^k	103.05 (7)	103.41 (9)
CaQ ₆		
Ca-Q (1) ^a	2.834 (3)	2.949 (4)
Ca-Q (2) ^b	2.791 (3)	2.908 (4)
Ca-Q (3) ^{c,d}	2.811 (2) (2×)	2.936 (3) (2×)
Ca-Q (3) ^{b,e}	2.890 (2) (2×)	2.990 (3) (2×)
Q (1) ^a -Ca-Q (2) ^b	169.37 (8)	170.4 (2)
Q (1) ^a -Ca-Q (3) ^{c,d}	90.76 (5) (2×)	90.3 (1) (2×)
Q (1) ^a -Ca-Q (3) ^{b,e}	79.06 (5) (2×)	80.00 (9) (2×)
Q (2) ^b -Ca-Q (3) ^{c,d}	96.53 (6) (2×)	96.35 (10) (2×)
Q (2) ^b -Ca-Q (3) ^{b,e}	93.06 (6) (2×)	93.0 (1) (2×)
Q (3) ^c -Ca-Q (3) ^d	93.14 (7)	91.3 (1)
Q (3) ^{c,d} -Ca-Q (3) ^{b,e}	90.91 (3) (2×)	90.97 (3) (2×)
Q (3) ^{c,d} -Ca-Q (3) ^{a,b}	169.10 (6) (2×)	170.1 (1) (2×)
Q (3) ^b -Ca-Q (3) ^e	83.39 (7)	85.2 (1)

^aSymmetry codes: a: x, y, z ; b: $x, y, 1 + z$; c: $1/2 - x, -y, 1/2 + z$; d: $1/2 - x, 1/2 + y, 1/2 + z$; e: $x, 1/2 - y, 1 + z$; f: $1/2 - x, -y, -1/2 + z$; g: $1/2 + x, 1/2 - y, 1/2 - z$; h: $1 - x, -1/2 + y, 1 - z$; i: $1/2 + x, y, 1/2 - z$; j: $-1/2 + x, 1/2 - y, 1/2 - z$; k: $x, 1/2 - y, z$. Note: the sum of the Shannon crystal radii for the six-coordinated Yb³⁺ (1.008 Å), Ca²⁺ (1.14 Å) and four coordinated In³⁺ (0.76 Å) with S²⁻ (1.70 Å) and Se²⁻ (1.84 Å) are 2.71 Å (Yb-S), 2.85 Å (Yb-Se), 2.46 Å (In-S), 2.60 Å (In-Se), 2.84 Å (Ca-S) and 2.98 Å (Ca-Se).²⁰

while the InQ₄ tetrahedra share cis edges with the octahedra, as shown in the middle slab of the polyhedral drawing the Figure 2. The neighboring octahedral chains in the same slab are connected by sharing every other bridging chalcogen atoms of the octahedra with the apical chalcogen atoms of the tetrahedra. The structure is arranged such that no significant Yb-Yb interaction should be expected, since the shortest separation is a half unit cell of *b* which is beyond the range of metal-metal bonding.

Conclusion

CaYbInQ₄ (Q = S and Se) represents a new family of ceramic materials that are potential candidates for LWIR optical applications. The thermal decomposition tem-

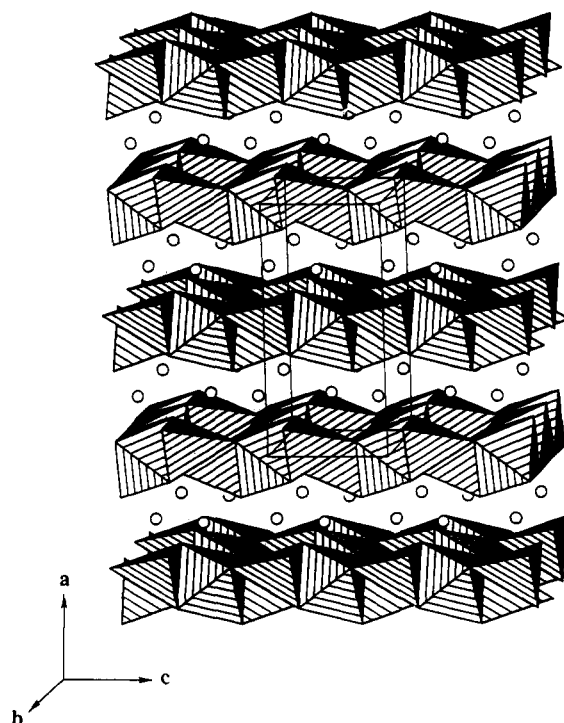


Figure 2. STRUPLO polyhedral drawing of the slab structure of CaYbInS₄. The [YbInQ₄]²⁻ slabs are stacked along the *a* axis with the calcium atoms (open circles) in between the slabs. The unit cell is outlined by solid lines.

peratures of the title compounds are higher than those found for the ternary post transition metal sulfides. This phenomenon is consistent with the previously studied ternary rare-earth chalcogenides, e.g. CdY₂S₄ (650 °C),² suggesting that the incorporation of rare-earth elements may give rise to an increased thermal stability. By using eutectic halide fluxes, our exploratory syntheses have proven to be fruitful in growing sufficiently sized single crystals of rare-earth element containing post-transition-metal chalcogenide compounds for structure and spectroscopy studies.

Acknowledgment. This research was supported by the Robert A. Welch Foundation and a Rice University startup grant. The authors are indebted to Mr. Z. Xiao for the DRIFTS experiments, to Mr. M. L. Pierson and Dr. J. C. Stormer, Jr. for WDS (funded by NSF), to Dr. S. Hsu (SHELL, Westhollow Research Center) for single-crystal IR spectroscopy, and Dr. Giuseppe L. Valderrama (HARC) for UV-vis spectroscopy. Financial support for the single-crystal X-ray diffractometer by the National Science Foundation is gratefully acknowledged.

Registry No. CaInYbS₄, 144126-44-3; CaInYbSe₄, 144126-45-4.

Supplementary Material Available: Table SI listing anisotropic thermal parameters (1 page); tables of calculated and observed structure factors (13 pages). Ordering information is given on any current masthead page.